

HOSTED BY

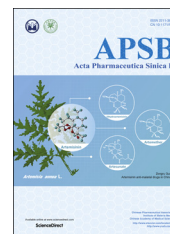


ELSEVIER

Chinese Pharmaceutical Association  
Institute of Materia Medica, Chinese Academy of Medical Sciences

Acta Pharmaceutica Sinica B

[www.elsevier.com/locate/apsb](http://www.elsevier.com/locate/apsb)  
[www.sciencedirect.com](http://www.sciencedirect.com)



REVIEW

# Injected nanocrystals for targeted drug delivery



Yi Lu<sup>a</sup>, Ye Li<sup>b</sup>, Wei Wu<sup>a,\*</sup>

<sup>a</sup>Department of Pharmaceutics, School of Pharmacy, Fudan University, Shanghai 201203, China

<sup>b</sup>Shaanxi Academy of Traditional Chinese Medicine, Xi'an 710003, China

Received 29 October 2015; received in revised form 4 November 2015; accepted 16 November 2015

## KEY WORDS

Nanocrystals;  
Targeted drug delivery;  
Biodistribution;  
Ligand;  
Stimuli response;  
Encapsulation

**Abstract** Nanocrystals are pure drug crystals with sizes in the nanometer range. Due to the advantages of high drug loading, platform stability, and ease of scaling-up, nanocrystals have been widely used to deliver poorly water-soluble drugs. Nanocrystals in the blood stream can be recognized and sequestered as exogenous materials by mononuclear phagocytic system (MPS) cells, leading to passive accumulation in MPS-rich organs, such as liver, spleen and lung. Particle size, morphology and surface modification affect the biodistribution of nanocrystals. Ligand conjugation and stimuli-responsive polymers can also be used to target nanocrystals to specific pathogenic sites. In this review, the progress on injected nanocrystals for targeted drug delivery is discussed following a brief introduction to nanocrystal preparation methods, *i.e.*, top-down and bottom-up technologies.

© 2016 Chinese Pharmaceutical Association and Institute of Materia Medica, Chinese Academy of Medical Sciences. Production and hosting by Elsevier B.V. This is an open access article under the CC BY-NC-ND license (<http://creativecommons.org/licenses/by-nc-nd/4.0/>).

\*Corresponding author. Tel.: +86 21 51980084.

E-mail address: [wuwei@shmu.edu.cn](mailto:wuwei@shmu.edu.cn) (Wei Wu).

Peer review under responsibility of Institute of Materia Medica, Chinese Academy of Medical Sciences and Chinese Pharmaceutical Association.

## 1. Introduction

More than 40% of drug candidates in the drug development process exhibit poor solubility, leading to poor and variable bioavailability<sup>1</sup>. The non-specific distribution of most drugs throughout the body results in side effects, further limiting their clinical use<sup>2</sup>. Targeting strategies based on nanocarriers are important solutions for these problems. Nanocarriers, *i.e.*, liposomes, nanoparticles, micelles and nanoemulsions, have been widely used to selectively deliver poorly soluble drugs to pathological tissues, organs or cells<sup>3</sup>. However, the intrinsic drawbacks, such as platform instability, limited drug loading, high manufacturing cost, scale-up difficulties, and quality control difficulties, contribute to the limited acceptance of these nanocarriers in clinic<sup>4</sup>. Only a couple of nanocarrier-based preparations are successfully marketed, *e.g.*, Doxil<sup>®</sup>, DaunoXome<sup>®</sup> and Abraxane<sup>®</sup>.

Development of nanocrystals emerged amid various shortcomings of existing delivery techniques for targeted therapy. Nanocrystals are drug crystals with particle size ranging from dozens to a few hundreds of nanometers, while in some cases, pure drug crystals may be physically stabilized by surfactants and/or polymers<sup>5–7</sup>. Absence of any carrier chemicals offer a theoretic drug loading up to 100%, typically 50%–90% (*w/w*)<sup>8</sup>, leading to satisfactory therapeutic concentrations at low dose<sup>9</sup>. Toxic side-effects resulting from the encapsulating/solubilizing excipients also may be eliminated. Most importantly, physical instability issues inherent with other nanocarriers are largely circumvented by the nanocrystal formulation<sup>10–12</sup>. In addition, both top-down and bottom-up technologies have been well developed to prepare nanocrystals with desired particle size and size distribution, while the ease of scaling-up for nanocrystals can be proved by a dozen of commercial products<sup>13</sup>.

Although invented for oral delivery to improve bioavailability of poorly soluble drugs, nanocrystals can be intravenously injected due to the nanoscale dimension. Due to lack of local mixing and initially insufficient volume of distribution, nanocrystals are not expected to dissolve rapidly in the blood upon *i.v.* administration, leading to improved biodistribution as compared to orally administered nanocrystals<sup>4</sup>. The injected nanocrystals are recognized as exogenous materials and sequestered by mononuclear phagocytic system (MPS) cells. Consequently, nanocrystals in the blood stream are passively targeted to organs in which MPS cells are abundant, such as liver and spleen<sup>14,15</sup>. It has been reported that the sequestering and transportation of exogenous particles by MPS cells is very fast and efficient. Up to 90% of the injected dose is transported to liver and about 5% to spleen within 5 min after injection<sup>9</sup>. The phagocytotic uptake by MPS cells is triggered by the adsorbance of opsonins from the blood onto the nanocrystal surface. Surface modification with hydrophilic polymers, such as polyethylene glycol (PEG) and poloxamer, can reduce opsonization and thus prolongs the circulating time of nanocrystals in blood, facilitating tumor accumulation through enhanced permeability and retention (EPR) effects<sup>9,16</sup>. The targeting efficiency of nanocrystals may be further improved using ligand modification<sup>17</sup>. Besides tumor sites, targeting to other pathogenic sites like inflammation can be achieved by adopting stimuli-response strategies<sup>16</sup>.

In this review, preparative methods for nanocrystals will be briefly introduced, followed by a detailed review on the progress of targeted drug delivery by nanocrystals. Polymer encapsulation to increase nanocrystal stability and immobilize ligands on the surface of nanocrystals will also be included.

## 2. Preparation of nanocrystals

### 2.1. Top-down techniques

High-energy mechanical forces are involved in the top-down approaches, which can be provided either by media milling (MM) (NanoCrystals<sup>®</sup>) or high-pressure homogenization (HPH) (IDD-P<sup>®</sup>, DissoCubes<sup>®</sup> and Nanopure<sup>®</sup>) to comminute large crystals<sup>14,15</sup>. The biggest advantage in top-down process is that it is a universal technique to prepare crystalline nanoparticles<sup>6</sup> and is flexible in production scale<sup>18</sup>. Thus, the process has been widely adopted to prepare commercial nanocrystals. Almost all commercial products were produced by NanoCrystals<sup>®</sup> except for Triglide<sup>®</sup> by IDD-P<sup>®</sup>. The disadvantage of this technology includes high energy and time consumption as well as contamination from the grinding media. For example, even with high pressure up to 1700 bar, 50–100 cycles of homogenization are still required to achieve the desired particle size and size distribution<sup>5,11</sup>; similarly, the milling time varies from hours to days, depending on the properties of the drug, the milling media, and the extent of particle size reduction<sup>19,20</sup>. Since contamination from the grinding media leads to unexpected side-effects, the top-down process may not be the optimal alternative to prepare nanocrystals for *i.v.* injection.

#### 2.1.1. Media milling (NanoCrystals<sup>®</sup>)

A milling chamber, motor, recirculating chamber, coolant and milling media are the major components of the media mill (Fig. 1). In the process, the milling chamber is fed with a crude slurry containing drug, water and stabilizers, and agitated by the motor. Generally, the slurry occupies 2%–30% (*w/v*) volume of the milling chamber, while the milling media occupy 10%–50% (*w/v*) of the slurry. During agitation, the milling media roll over inside the chamber, generating high energy forces by shearing and impacting with drugs to reduce the particle size. The operation can be performed either in batch (discontinuous mode) or recirculation mode (continuous mode), depending on the scale. Recirculation is advantageous to reduce milling time and decrease particle size. The milling media can be retained in the chamber by media separators if recirculation mode is performed. Thermogenesis is severe due to the high energy generated during milling and long-term operation, leading to stability concerns. Therefore, the coolant is a necessity to control the temperature during the milling process.

#### 2.1.2. High pressure homogenization (IDD-P<sup>®</sup>, DissoCubes<sup>®</sup> and Nanopure<sup>®</sup>)

During the process of HPH, drug suspensions are introduced into a high pressure homogenizer and forced to pass through a very narrow homogenization pathway in a sudden burst under high pressure (Fig. 2). Fracture of drug particles is achieved by cavitation, high-shear forces and collisions among particles. The process is generally composed of three steps: (1) dispersion of crude drug powders in pure solution or in solution containing stabilizer, (2) reduction of particle size by high-speed shearing or homogenization under low pressures, (3) high pressure homogenization to achieve the desirable particle size and size distribution. Based on the instruments and solution used, HPH can be further divided into three patented technologies: microfluidizer for IDD-P<sup>®</sup> technology, piston gap homogenizer for DissoCubes<sup>®</sup> (water) and Nanopure<sup>®</sup> (non-aqueous media).

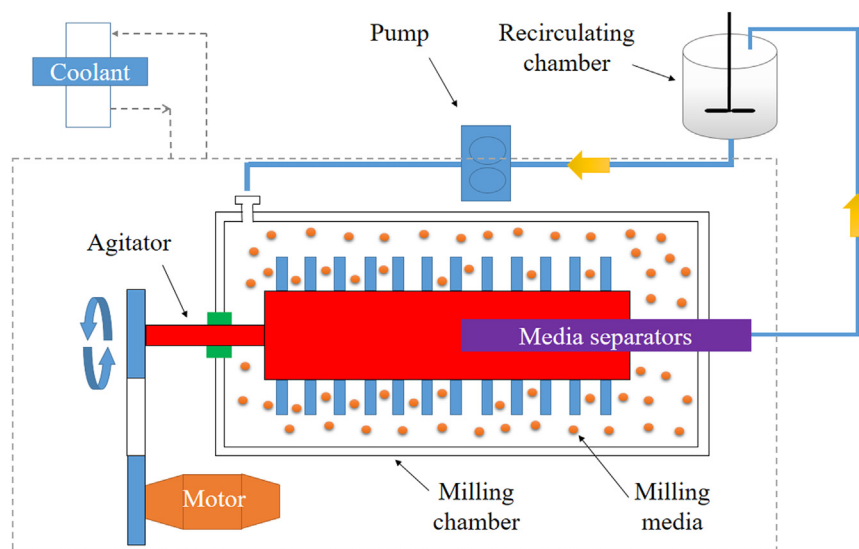


**Figure 1** Illustration of the media milling process. A crude slurry consisting of drug, water and stabilizer is fed into the milling chamber, which is agitated by a motor. The particle size of drug powders is reduced by shearing forces and impaction between milling media and drug. Recirculation can increase the milling efficiency, while the coolant can control the temperature of the materials. The milling time required to generate nanocrystals depends on the properties of the drugs, the milling media and the extent of particle size reduction, varying from hours to days.

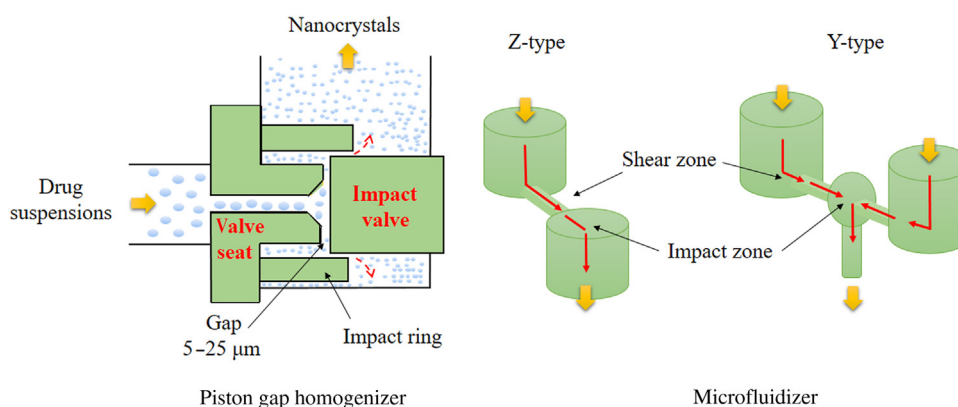


**Figure 2** Illustration of the high pressure homogenization process. Pretreated drug suspensions are forced through a tiny gap or specially designed homogenization chamber (Z- or Y- type) under high pressure, typically 1500–2000 bar. During this process, cavitation generated by high streaming velocity, together with high shear forces and collisions among particles, comminute big drug crystals to nanocrystals. A high number of passes, such as 50–100 passes, is still required even under 1700 bar to obtain the desirable particle size and size distribution.

## 2.2. Bottom-up techniques

The bottom-up process grows nanocrystals from solution, which includes two crucial steps: nucleation and consequent crystal growth. In comparison, nucleation is especially important to achieve small and uniform nanocrystals. Higher nucleation rate increases the number of nuclei formed from the supersaturated solution, leading to decreased supersaturation. Less growth of each nucleus in the end can be anticipated as a consequence<sup>21</sup>. Also, if a large number of nuclei are produced concurrently in the nucleation stage, a narrow particle size distribution is obtained<sup>21</sup>. Therefore, it is essential to promote rapid and homogeneous nucleation in the bottom-up process.

Nucleation can be triggered by either mixing with antisolvent or removal of solvent<sup>21,22</sup>. The mixing of drug solution and antisolvent is generally achieved with conventional mixing equipment, *i.e.* magnetic stirring and agitator blade<sup>23</sup>. In order to promote the

nucleation, sonication can be introduced to provide cavitation effects (Fig. 3)<sup>24,25</sup>. This method is called sonoprecipitation. Some highly efficient mixing equipments have also been used to prepare nanocrystals, including confined impinging jet reactor<sup>26–30</sup>, multiple inlet vortex mixer<sup>31</sup> and static mixer<sup>32</sup>. With these instruments, intense micro-mixing between the two fluids is fulfilled in the order of milliseconds<sup>33,34</sup>. A homogeneous solution with high supersaturation may be achieved even before the onset of nucleation, favoring small nanocrystals with narrow size distribution. Spray-drying and freeze-drying are common ways to remove solvent. Recently, spray-freezing into liquid<sup>35–38</sup> and controlled crystallization during freeze-drying techniques<sup>39</sup> also has been developed to prepare nanocrystals by removal of solvent.

Supercritical fluid (SCF) can be used to prepare nanocrystals by taking advantage of the unique physical properties of SCF, with combined diffusivity like gas and solubilization like liquid. In addition, quick and easy removal of SCF without excessive drying can greatly

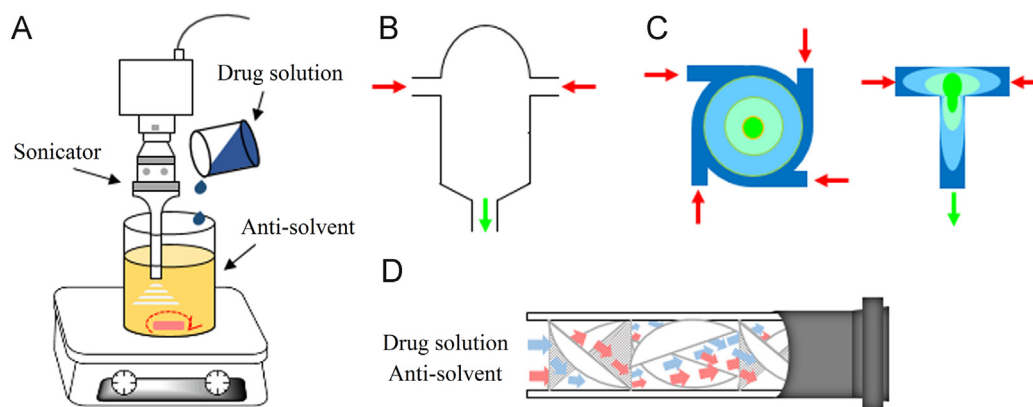


**Figure 3** Schematic illustration of bottom-up techniques in which crystallization is triggered by solvent/anti-solvent mixing. Sonication can be combined with a common mixing instrument such as magnetic stirring to promote nucleation (A). With highly efficient mixing equipment, including confined impinging jet reactor (B), multiple inlet vortex mixer (C) and static mixer (D), intense micro-mixing may be achieved even before the onset of nucleation, favoring small and homogeneous nanocrystals.

facilitate the precipitation of nanoparticles. Supercritical carbon dioxide ( $\text{SCO}_2$ ) is the most favored SCF due to the mild critical point (31 °C and 73.8 bar) and low environmental impact. Depending on the solubility of a compound in  $\text{SCO}_2$ , nanocrystal preparation can be achieved by rapid expansion of  $\text{SCO}_2$  from drug solution<sup>40</sup>, or by precipitation using  $\text{SCO}_2$  as the antisolvent<sup>41–43</sup>.

### 3. Targeted delivery by nanocrystals

#### 3.1. *In vivo* distribution of nanocrystals

Due to being sequestered and transported by MPS cells, i.v. injected nanocrystals distribute more in MPS cell-abundant organs, such as liver, spleen and lung, than the solution counterpart<sup>4,14,15</sup>. Nevirapine nanocrystals are more easily taken up *in vitro* by macrophages than the solution formulation, showing 2.76-fold higher nevirapine concentration in macrophages at the end of a two-hour culture. Therefore, gamma scintigraphy confirmed that nevirapine nanocrystals accumulated more in MPS-rich organs including spleen, liver and thymus, as well as exhibited prolonged residence at the target sites in comparison to pure drug solution<sup>44</sup>. Similarly, the relative targeting efficacy ( $r_c^e$ ) values of liver, lung and spleen for amoitone B nanocrystals (275 nm) are 3.32, 2.50 and 1.42, respectively, compared to the solution (Table 1<sup>44–52</sup>). The nanocrystals remained in liver and lung for a longer time, benefiting therapy in liver and lung<sup>45,46</sup>. Indeed, hydroxycamptothecin nanocrystals (168 nm) were highly accumulated in liver, spleen and lung<sup>47</sup>. The area under curve (AUC) of hydroxycamptothecin nanocrystals in liver, spleen and lung respectively are 410-, 46- and 40- fold higher than that obtained with a solution formulation (Table 1).

Particle size may play a significant role in the biodistribution of nanocrystals. Oridonin nanocrystals were prepared by HPH, with mean particle size of 103 nm and 897 nm achieved by adjusting the homogenization pressure. The more finely ground sample showed similar biodistribution to the solution, as indicated by the  $r_c^e$  values in all tested organs around 1 (Table 1). However, the cruder preparation showed different biodistribution characteristics. Highest accumulation was observed in liver with  $r_c^e$  values of 8.82, followed by spleen of 7.79 and lung of 3.23 (Table 1)<sup>48</sup>. Similar distribution characteristics were observed for i.v. injected riccardin D nanocrystals with different

particle sizes<sup>49</sup>. As described by the Ostwald-Freundlich equation, nanocrystals exhibit nonlinear increase in kinetic solubility upon particle size reduction<sup>53</sup>. It is thus hypothesized that the smaller nanocrystals dissolve relatively quickly in blood, minimizing phagocytosis by the MPS cells and presenting similar *in vivo* behavior to the solution<sup>17</sup>. On the contrary, larger particles are more likely to be phagocytosed by the MPS, resulting in greater distribution to liver, spleen and lung<sup>48,49</sup>. The size effects on biodistribution are still controversial. Asulacrine nanocrystals, 133 nm, were prepared by HPH. Although having enhanced dissolution and saturation solubility, the nanocrystals still showed a significantly greater accumulation in liver, lung and kidney with altered pharmacokinetics, as compared to the solution<sup>54</sup>. AZ68 amorphous nanosuspensions, 100–150 nm, showed enhanced oral bioavailability over the crystalline nanocrystals, 300–400 nm, due to enhanced solubility and dissolution rate. However, no significant difference was found in the pharmacokinetic parameters when comparisons were made between the formulations after i.v. administration<sup>55</sup>. Nanocrystals are usually adopted by insoluble drugs. Given the insoluble properties (usually <0.1 mg/mL), especially for anticancer drugs<sup>56</sup>, combined with high i.v. dose, injected nanocrystals are not expected to dissolve rapidly due to lack of local mixing and insufficient initial volume for distribution<sup>4</sup>.

Particle morphology also influences the biodistribution of nanocrystals. Spherical and rod-like 10-hydroxycamptothecin nanocrystals (500 nm) were prepared with similar hydrodynamic sizes and surface charges<sup>57</sup>. The rod-like nanocrystals showed significantly higher uptake by KB cells than the spherical ones. Therefore a shape-dependent cytotoxicity was observed. In addition, *in vivo* studies showed obviously superior antitumor efficacy was achieved by the rod-like nanocrystals over the spherical one and free drug solution, and no statistically significant weight loss was observed. Similarly, the needle-shaped camptothecin nanocrystals (250 nm) accumulated more in the lung, because the high aspect ratio may hinder the escape from local entrapment<sup>58</sup>.

Surface modification of nanocrystals may change their biodistribution behaviors. Serum albumin, PEG and dextran was physically adsorbed on the surface of nevirapine nanocrystals by simply incubating the bare nanocrystals in the modifier solution<sup>50</sup>. Surface modification with PEG reduced the uptake of nanocrystals by primary macrophages. On the contrary, surface modification with serum albumin and dextran showed 1.39 and 1.22 fold higher cellular drug

**Table 1** Biodistribution properties of i.v. injected nanocrystals and factors affecting biodistribution.

Drug	Stabilizer	Size (nm)	Animal model	Reference preparation	Biodistribution ( $r_c^{ca}$ )								Ref.
					Blood	Heart	Liver	Spleen	Lung	Kidney	Tumor	Thymus	
Am-B	PC/F68	275	Mice	Solution	2.07	0.77	3.32	1.42	2.50	0.82			45,46
HCPT	None	168	H22 bearing mice	Solution	8.78	7.01	410.49	46.05	40.63	42.03	5.72		47
Effects of particle size on the biodistribution													
ORI	F68/PC	103	Mice	Solution	1.05	1.09	0.97	0.88	1.09	1.05			48
		897			2.44	1.25	8.82	7.79	3.23	1.59			
RD	F68/PVP/HPMC	184	Mice	Solution	0.40	0.89	1.33	2.65	1.08	1.43			49
		815			0.93	1.29	2.34	3.71	4.98	1.48			
Effects of surface modification on the biodistribution													
NVP	None	458	Rats	Solution	1.75	1.16	1.77	2.56	0.62	0.75		4.22	44,50
	Serum albumin	495		Solution	1.02	0.60	2.60	3.74	4.75	0.57		6.21	
				Bare nanocrystals	0.58	0.52	1.47	1.46	7.66	0.76		1.47	
	PEG	520		Solution	1.86	1.36	2.65	2.82	2.19	0.85		3.46	
				Bare nanocrystals	1.06	1.17	1.50	1.10	3.53	1.13		0.82	
	Dextran	520		Solution	1.14	0.86	2.51	2.80	2.27	0.54		4.36	
				Bare nanocrystals	0.65	0.74	1.42	1.09	3.66	0.72		1.03	
Effects of ligand conjugation on biodistribution													
PIK-75	PC/F68	182	SKOV-3 bearing Mice	Solution			0.77	13.76	0.91	0.72	4.69		51
	PC/FA-F68	161					0.80	15.90	0.82	0.38	8.90		
DTX	PC/DSPE-PEG	204	B16 bearing mice	Solution		0.97	17.86	9.80	3.23	0.93	5.22		52
	PC/DSPE-PEG-FA	221				0.96	17.14	9.97	3.37	0.95	5.92		

Am-B, amoitone B; DTX, docetaxel; F68, Pluronic F68; FA, folic acid; HCPT, hydroxycamptothecin; NVP, nevirapine; ORI, oridonin; PC, phosphatidylcholine; RD, riccardin D.

<sup>a</sup>Relative efficiency, calculated by the AUC value of the tested preparation divided by that of the reference preparation.

concentration at the end of 2 h than that of bare nanocrystals. As a consequence, surface modification with serum albumin and dextran decreased the accumulation of bare nanocrystals in blood, while increased accumulation in liver, spleen and lung, both due to fast uptake by macrophages. Furthermore, the nevirapine nanocrystals were able to cross blood-brain barrier in less than 30 min and maintained adequate levels up to 24 h after modification with serum albumin. None of the other nanocrystals formulations, modified or not, showed significant levels in brain. Polycations, including IgG, protamine and 1,2-dioleoyl-3-trimethylammonium-propane (DOTAP), were once used to coat the bare paclitaxel (PTX) nanocrystals by physical adsorption<sup>59</sup>. DOTAP-coated nanocrystals (DOTAP-NCs) showed faster *in vitro* macrophage uptake than other coated and bare nanocrystals, especially by immature CD14<sup>+</sup>CD16<sup>-</sup> cells relative to mature CD14<sup>+</sup>CD16<sup>+</sup> cells. The cellular uptake rate was in accordance with the sequence of positive charge. On the contrary, the IgG-coated nanocrystals were more preferentially taken up by the CD14<sup>+</sup>CD16<sup>+</sup> monocyte subset class due to binding of IgG to FcγR-III receptor on CD16<sup>+</sup>. Additionally, DOTAP-coated nanocrystals were taken up more readily by peritoneal macrophages and OVCAR-3 cancer cells than were uncoated nanocrystals. Subsequent experiments *in vivo* suggested that DOTAP-coated nanocrystals could be trafficked preferentially to the tumor site by macrophages<sup>59</sup>.

Direct evidence showing *in vivo* macrophage uptake and transportation of nanocrystals is still missing. Instead, there are numerous speculations from the altered pharmacokinetics, involving

lower  $C_{max}$  and longer  $t_{1/2}$ , due to slow release from the deposition of macrophages. A transmission electron micrograph of spleen from a rat that received i.v. injection of itraconazole nanocrystals once showed crystalline materials in the macrophages<sup>60</sup>. Although the crystalline materials were attributed to itraconazole nanocrystals, they may be resulted from the recrystallization of itraconazole molecules during sample preparation, because ethanol was used for dehydration before resin section. Cryo-TEM may be a good alternative to study the *in vivo* fate of nanocrystals.

### 3.2. Ligand targeted delivery

To facilitate targeting to cancer cells, the strategy of using various ligands that bind specifically to a receptor expressed by malignant cells is attractive. Attaching ligands to the surface of nanocrystals can thus deliver the drug specifically to the cancer cell *via* receptor-mediated endocytosis with minimal accumulation at nonspecific sites. Note that modification with “stealth” molecules like PEG and poloxamer to avoid quick clearance by macrophages is still essential.

Folate-based targeting systems present an effective means of selectively delivering therapeutic agents to tumors, because the folate receptor is overexpressed on many human cancer cells, folate has low immunogenicity, its ease of modification, good tissue penetration and rapid clearance from receptor-negative tissues. Folate-modified PIK-75 (a phosphatidylinositol 3-kinase inhibitor) nanocrystals were prepared by HPH with Pluronic F68-folate



conjugate as the stabilizer<sup>51</sup>. Folate modification was achieved through physical adsorption of Pluronic F68 on the surface of the nanocrystals. The folate-modified nanocrystals showed a 1.8-fold and 1.4-fold higher PIK-75 concentration in SKOV-3 cells at 1 h and 6 h of incubation respectively compared to nanocrystals without folate modification. Both nanocrystals showed similar distribution in liver, kidney, spleen and lung. However, the folate-modified nanocrystals increased their AUC by 1.90-fold at the tumor site compared to non-modified nanocrystals (Table 1).

Ligand modification will not always increase the tumor distribution of nanocrystals. Folate conjugated with distearoylphosphatidyl ethanolamine-PEG2000 (DSPE-PEG2000-FA) was used to coat docetaxel nanocrystals<sup>52</sup>. The folate-modified nanocrystals showed increased cellular toxicity as compared to nonfolate-modified nanocrystals in folate receptor positive cell lines (B16 cells), and was attributed to folate-induced internalization by the target cells. In contrast, both nanocrystals showed similar *in vivo* distribution in B16 tumor-bearing mice including the tumor sites (Table 1). Instead of being chemically anchored, the ligands are reversibly adsorbed onto the surface of nanoparticles through stabilizers. Although equilibrium can be reached between adsorbance and desorption in solution, stabilizers can be detached from nanocrystals upon mild heating or dilution<sup>61</sup>, inevitably resulting in loss of the stabilizing agent as well as any appended ligands by *in vivo* dilution. Furthermore, the binding between ligands and receptors on the surfaces of the target sites may be preferential over the adsorbance between stabilizers and nanocrystals, leading to the binding of ligands alone to the receptors<sup>62</sup>.

### 3.3. Stimuli-responsive drug delivery

Generally, stabilizer adsorbed onto the surface of nanocrystals can prevent aggregation by providing steric and/or electronic repulsions. An optimal surfactant thus should have high affinity to the surface of nanocrystals. But in some cases, shedding of the stabilizer in response to a local endogenous stimulus may in fact be beneficial. For instance, shedding of D- $\alpha$ -tocopheryl polyethylene glycol 1000 succinate (TPGS) from the paclitaxel nanocrystals improved the toxicity to multidrug resistant cells by inhibiting P-glycoprotein (P-gp)<sup>63</sup>. Polymers that undergo physicochemical changes in response to environmental stimuli such as temperature, pH, magnetic field or enzymes have been widely used for drug delivery. Adoption of these stimuli-responsive polymers as stabilizers may allow nanocrystals to accumulate at sites of disease.

Reactive oxygen species (ROS) are strongly associated with and limited to inflammation and cancer sites, stimulating investigations of ROS-sensitive drug delivery systems<sup>64–66</sup>. A library of 10 redox-responsive amphiphilic block copolymers was prepared by post-polymerization modification using the thiol-yne reaction<sup>8</sup>. The hydrophobic thiol agents grafted to the polymer endowed these copolymers with good stabilizing effects to prepare paclitaxel nanocrystals with mean diameters of around 200 nm. Oxidation of the thioether side chain to a sulfoxide or sulfone significantly alters the polarity of the hydrophobic block, leading to desorption of the copolymers from the surface of the nanocrystals. Compared to other ROS sensitive systems, the prepared copolymers are more sensitive to H<sub>2</sub>O<sub>2</sub> (as low as 100  $\mu$ mol/L) and respond relatively quickly (within 2 h). The redox-responsive copolymers may pave the way for the design of ROS-sensitive drug delivery systems by location-specific shedding of stabilizers, which can be used for imaging or improving cellular uptake.

The pH at pathological sites, involving inflammation, infection or tumors, is lower than that of the normal tissues, which can be exploited to achieve site-specific activation of many pharmaceutical and

therapeutic agents<sup>67</sup>. Calcium carbonate (CaCO<sub>3</sub>) nanocrystals were synthesized in oil-in-water microemulsions using a high pressure homogenizer to deliver doxorubicin (CaCO<sub>3</sub>/Dox nanocrystals)<sup>68</sup>. CaCO<sub>3</sub>/Dox nanocrystals showed a pH-dependent Dox release pattern, *i.e.* slow release at normal physiological pH value (7.4) while a fast release at acidic pH value (4.8) simulating tumor microenvironment. The cellular experiments further indicated that CaCO<sub>3</sub>/Dox nanocrystals are promising materials in the delivery of anticancer drugs.

## 4. Encapsulation of nanocrystals

As discussed above, stabilizers are generally reversibly adsorbed onto the surfaces of drug nanocrystals, being easily shed from the nanocrystals by dilution or heating. The desorption of stabilizers may cause stability concerns or even affect the *in vivo* performance of nanocrystals. An improvement for this issue is to encapsulate nanocrystals in cages.

The layer-by-layer (LbL) assemble technique is an effective way to stabilize particles, based on the iterative adsorption of oppositely charged polymers on a surface<sup>23</sup>. Compared with the one-layer physisorption of stabilizers, the iterative coating may provide a firm shell to stabilize nanocrystals. Tamoxifen (TMF) and paclitaxel (PTX) nanocrystals (between 100 nm and 200 nm) can be stabilized by the LbL assembly technique with positively charged poly(allylamine hydrochloride) (PAH), poly (dimethyldiallylamide ammonium chloride) (PDDA), and negatively charged sodium poly (styrene sulfonate) (PSS), respectively<sup>69</sup>. LbL coating did not significantly alter the particle sizes and morphologies of nanocrystals, while drug release can be easily controlled by changing the coating thickness or composition. Furthermore, with polyamino-containing PAH as the outer layer, the specific targeting ligands such as mAb 2C5 can be conjugated to LbL-stabilized PTX nanocrystals, leading to increased cytotoxicity to MCF-7 and BT-20 cells.

Cross-linking of stabilizers adsorbed onto the surface of nanocrystals is another option to avoid shedding of stabilizers. Chitosan was used as a stabilizer to prepare PTX nanocrystals by media milling, followed by immobilization onto the surface of the nanocrystals through cross-linking with tripolyphosphate<sup>62</sup>. Furthermore, folate was introduced to the surface of the cross-linked chitosan/drug nanocrystals by conjugation through *N*-(3-dimethylaminopropyl)-*N'*-ethylcarbodiimide hydrochloride (EDC). The cross-linked chitosan, acting as a diffusion barrier, decreased the release of PTX, while conjugation further decreased the release due to the reinforced hydrophobicity by folate. Cross-linking by click chemistry can also be used to encapsulate nanocrystals. Amphiphilic copolymer was synthesized by ring-opening copolymerization with mPEG as a hydrophilic segment to provide steric stabilizing effects and alkynyl containing poly( $\delta$ -valerolactone) as hydrophobic segment to adsorb on to PTX nanocrystals<sup>70</sup>. The adsorbed copolymer can be crosslinked by diazido-containing molecules through click chemistry around nanocrystals, forming a non-sheddable polymeric “nanocage”. The nanocages were found to act as sterically stabilizing barriers to prevent aggregation and provided a means for enhanced retention of targeting agents on nanocrystals. Although all of the abovementioned cross-linked nanocrystals show potential in improved stability and targetability, biodistribution and cellular uptake studies have not been reported.

## 5. Summary and future perspective

Compared with traditional nanocarriers, the advantages of nanocrystals in physical stability, high drug loading and relative ease of

production bring attractive alternatives for delivery of poorly soluble drugs. Both top-down and bottom-up techniques have been developed for preparing nanocrystals. The bottom-up techniques may be more suitable to prepare nanocrystals for i.v. injection than the top-down techniques, considering the potential contamination from milling media.

Due to quick ingestion by macrophages, the i.v. injected nanocrystals can be passively delivered to MPS rich organs, such as liver, spleen and lung. Particle size, morphology and surface modification may greatly influence the *in vivo* distribution of nanocrystals. Although ligands facilitate targeting to cancer cells, physically adsorbed ligands on the surface of nanocrystals may be shed by dilution *in vivo*, losing the targeting function. However, shedding of stabilizers in response to pH or oxygen may be advantageous for targeted delivery to some specific pathogenic sites like tumors or sites of inflammation. Furthermore, stabilizers can be immobilized on the surface of nanocrystals by crosslinking, which may enhance not only the stability of nanocrystals but also retention of targeting agents.

However, both the *in vitro* cellular uptake and the *in vivo* fate of nanocrystals have not been fully explored due to the limitation of current detection technologies. The cellular uptake and *in vivo* distribution of nanocrystals is generally detected by measuring the amount of drug molecule present. It is difficult to discriminate if the results are due to the nanocrystals themselves or the dissolved molecules. Hybrid nanocrystals, by physically integrating fluorescent dyes inside the crystal<sup>71–73</sup>, may be a good way to resolve this issue. Only with complete understanding of the factors that affect the performance of nanocrystals can an optimal formulation be designed. In addition, with breakthroughs in the development of novel methods and devices, we believe that i.v. injected nanocrystals will occur in the near future.

## References

1. Ranjita S. Nanosuspensions: a new approach for organ and cellular targeting in infectious diseases. *J Pharm Invest* 2013;**43**:1–26.
2. Trapani G, Denora N, Trapani A, Laquintana V. Recent advances in ligand targeted therapy. *J Drug Target* 2012;**20**:1–22.
3. Hollis CP, Zhao R, Li T. Hybrid nanocrystal as a versatile platform for cancer theranostics. In: Park K, editor. *Biomaterials for cancer therapeutics: diagnosis, prevention and therapy*. Cambridge: Woodhead Publishing; 2013. p. 186–204.
4. Lu Y, Chen Y, Gemeinhart RA, Wu W, Li T. Developing nanocrystals for cancer treatment. *Nanomedicine (Lond)* 2015;**10**:2537–52.
5. Keck CM, Muller RH. Drug nanocrystals of poorly soluble drugs produced by high pressure homogenisation. *Eur J Pharm Biopharm* 2006;**62**:3–16.
6. Rabinow BE. Nanosuspensions in drug delivery. *Nat Rev Drug Discov* 2004;**3**:785–96.
7. Xu Y, Liu X, Lian R, Zheng S, Yin Z, Lu Y, et al. Enhanced dissolution and oral bioavailability of aripiprazole nanosuspensions prepared by nanoprecipitation/homogenization based on acid-base neutralization. *Int J Pharm* 2012;**438**:287–95.
8. Fuhrmann K, Polomska A, Aeberli C, Castagner B, Gauthier MA, Leroux JC. Modular design of redox-responsive stabilizers for nanocrystals. *ACS Nano* 2013;**7**:8243–50.
9. Muller RH, Gohla S, Keck CM. State of the art of nanocrystals—special features, production, nanotoxicology aspects and intracellular delivery. *Eur J Pharm Biopharm* 2011;**78**:1–9.
10. Chen H, Khemtong C, Yang X, Chang X, Gao J. Nanonization strategies for poorly water-soluble drugs. *Drug Discov Today* 2011;**16**:354–60.
11. Junghanns JU, Muller RH. Nanocrystal technology, drug delivery and clinical applications. *Int J Nanomed* 2008;**3**:295–309.
12. Guo S, Huang L. Nanoparticles containing insoluble drug for cancer therapy. *Biotechnol Adv* 2014;**32**:778–88.
13. Nagarwal RC, Kumar R, Dhanawat M, Das N, Pandit JK. Nanocrystal technology in the delivery of poorly soluble drugs: an overview. *Curr Drug Deliv* 2011;**8**:398–406.
14. Shegokar R, Muller RH. Nanocrystals: industrially feasible multi-functional formulation technology for poorly soluble actives. *Int J Pharm* 2010;**399**:129–39.
15. Merisko-Liversidge E, Liversidge GG, Cooper ER. Nanosizing: a formulation approach for poorly-water-soluble compounds. *Eur J Pharm Sci* 2003;**18**:113–20.
16. Fuhrmann K, Gauthier MA, Leroux JC. Targeting of injectable drug nanocrystals. *Mol Pharm* 2014;**11**:1762–71.
17. Gao L, Liu G, Ma J, Wang X, Zhou L, Li X. Drug nanocrystals: *in vivo* performances. *J Control Release* 2012;**160**:418–30.
18. Muller RH, Jacobs C, Kayser O. Nanosuspensions as particulate drug formulations in therapy. Rationale for development and what we can expect for the future. *Adv Drug Deliv Rev* 2001;**47**:3–19.
19. Gao L, Zhang D, Chen M. Drug nanocrystals for the formulation of poorly soluble drugs and its application as a potential drug delivery system. *J Nanopart Res* 2008;**10**:845–62.
20. Peltonen L, Hirvonen J. Pharmaceutical nanocrystals by nanomilling: critical process parameters, particle fracturing and stabilization methods. *J Pharm Pharmacol* 2010;**62**:1569–79.
21. Hollis CP, Li T. Nanocrystals production, characterization, and application for cancer therapy. In: Yeo Y, editor. *Nanoparticulate drug delivery systems: strategies, technologies, and applications*. New York: John Wiley & Sons, Inc; 2013. p. 181–206.
22. de Waard H, Frijlink HW, Hinrichs WL. Bottom-up preparation techniques for nanocrystals of lipophilic drugs. *Pharm Res* 2011;**28**:1220–3.
23. Xia D, Gan Y, Cui F. Application of precipitation methods for the production of water-insoluble drug nanocrystals: production techniques and stability of nanocrystals. *Curr Pharm Des* 2014;**20**:408–35.
24. Dalvi SV, Yadav MD. Effect of ultrasound and stabilizers on nucleation kinetics of curcumin during liquid antisolvent precipitation. *Ultrason Sonochem* 2015;**24**:114–22.
25. Dalvi SV, Dave RN. Analysis of nucleation kinetics of poorly water-soluble drugs in presence of ultrasound and hydroxypropyl methyl cellulose during antisolvent precipitation. *Int J Pharm* 2010;**387**:172–9.
26. D'Addio SM, Prud'homme RK. Controlling drug nanoparticle formation by rapid precipitation. *Adv Drug Deliv Rev* 2011;**63**:417–26.
27. Dong Y, Ng WK, Shen S, Kim S, Tan RBH. Controlled antisolvent precipitation of spironolactone nanoparticles by impingement mixing. *Int J Pharm* 2011;**410**:175–9.
28. Beck C, Dalvi SV, Dave RN. Controlled liquid antisolvent precipitation using a rapid mixing device. *Chem Eng Sci* 2010;**65**:5669–75.
29. Siddiqui SW, Unwin PJ, Xu Z, Kresta SM. The effect of stabilizer addition and sonication on nanoparticle agglomeration in a confined impinging jet reactor. *Colloid Surf A* 2009;**350**:38–50.
30. Chiou H, Chan HK, Prud'homme RK, Raper JA. Evaluation on the use of confined liquid impinging jets for the synthesis of nanodrug particles. *Drug Dev Ind Pharm* 2008;**34**:59–64.
31. Liu Y, Cheng C, Liu Y, Prud'homme RK, Fox RO. Mixing in a multi-inlet vortex mixer (MIVM) for flash nano-precipitation. *Chem Eng Sci* 2008;**63**:2829–42.
32. Alvarez AJ, Myerson AS. Continuous plug flow crystallization of pharmaceutical compounds. *Cryst Growth Des* 2010;**10**:2219–28.
33. Han J, Zhu Z, Qian H, Wohl AR, Beaman CJ, Hoyer TR, et al. A simple confined impingement jets mixer for flash nanoprecipitation. *J Pharm Sci* 2012;**101**:4018–23.
34. Lince F, Bolognesi S, Marchisio DL, Stella B, Dosio F, Barresi AA, et al. Preparation of poly(MePEGCA-co-HDCA) nanoparticles with confined impinging jets reactor: experimental and modeling study. *J Pharm Sci* 2011;**100**:2391–405.

35. Hu J, Rogers TL, Brown J, Young T, Johnston KP, Williams RO 3rd. Improvement of dissolution rates of poorly water soluble APIs using novel spray freezing into liquid technology. *Pharm Res* 2002;**19**:1278–84.
36. Rogers TL, Nelsen AC, Hu J, Brown JN, Sarkari M, Young TJ, et al. A novel particle engineering technology to enhance dissolution of poorly water soluble drugs: spray-freezing into liquid. *Eur J Pharm Biopharm* 2002;**54**:271–80.
37. Rogers TL, Hu J, Yu Z, Johnston KP, Williams RO 3rd. A novel particle engineering technology: spray-freezing into liquid. *Int J Pharm* 2002;**242**:93–100.
38. Hu J, Johnston KP, Williams RO 3rd. Spray freezing into liquid (SFL) particle engineering technology to enhance dissolution of poorly water soluble drugs: organic solvent *versus* organic/aqueous co-solvent systems. *Eur J Pharm Sci* 2003;**20**:295–303.
39. de Waard H, Hinrichs WL, Frijlink HW. A novel bottom-up process to produce drug nanocrystals: controlled crystallization during freeze-drying. *J Control Release* 2008;**128**:179–83.
40. Tuerk M. Manufacture of submicron drug particles with enhanced dissolution behaviour by rapid expansion processes. *J Supercrit Fluid* 2009;**47**:537–45.
41. Reverchon E, De Marco I, Torino E. Nanoparticles production by supercritical antisolvent precipitation: a general interpretation. *J Supercrit Fluid* 2007;**43**:126–38.
42. Kim MS, Jin SJ, Kim JS, Park HJ, Song HS, Neubert RHH, et al. Preparation, characterization and *in vivo* evaluation of amorphous atorvastatin calcium nanoparticles using supercritical antisolvent (SAS) process. *Eur J Pharm Biopharm* 2008;**69**:454–65.
43. Zhao X, Zu Y, Li Q, Wang M, Zu B, Zhang X, et al. Preparation and characterization of camptothecin powder micronized by a supercritical antisolvent (SAS) process. *J Supercrit Fluid* 2010;**51**:412–9.
44. Shegokar R, Singh KK. Nevirapine nanosuspensions for HIV reservoir targeting. *Pharmazie* 2011;**66**:408–15.
45. Hao L, Luan J, Zhang D, Li C, Guo H, Qi L, et al. Research on the *in vitro* anticancer activity and *in vivo* tissue distribution of Amoitone B nanocrystals. *Coll Surf B* 2014;**117**:258–66.
46. Hao L, Wang X, Zhang D, Xu Q, Song S, Wang F, et al. Studies on the preparation, characterization and pharmacokinetics of Amoitone B nanocrystals. *Int J Pharm* 2012;**433**:157–64.
47. Han M, Liu X, Guo Y, Wang Y, Wang X. Preparation, characterization, biodistribution and antitumor efficacy of hydroxycamptothecin nanosuspensions. *Int J Pharm* 2013;**455**:85–92.
48. Gao L, Zhang D, Chen M, Duan C, Dai W, Jia L, et al. Studies on pharmacokinetics and tissue distribution of oridonin nanosuspensions. *Int J Pharm* 2008;**355**:321–7.
49. Liu G, Zhang D, Jiao Y, Guo H, Zheng D, Jia L, et al. *In vitro* and *in vivo* evaluation of riccardin D nanosuspensions with different particle size. *Coll Surf B* 2013;**102**:620–6.
50. Shegokar R, Singh KK. Surface modified nevirapine nanosuspensions for viral reservoir targeting: *in vitro* and *in vivo* evaluation. *Int J Pharm* 2011;**421**:341–52.
51. Talekar M, Ganta S, Amiji M, Jamieson S, Kendall J, Denny WA, et al. Development of PIK-75 nanosuspension formulation with enhanced delivery efficiency and cytotoxicity for targeted anti-cancer therapy. *Int J Pharm* 2013;**450**:278–89.
52. Wang L, Li M, Zhang N. Folate-targeted docetaxel-lipid-based-nanosuspensions for active-targeted cancer therapy. *Int J Nanomed* 2012;**7**:3281–94.
53. Shchekin AK, Rusanov AI. Generalization of the Gibbs-Kelvin-Kohler and Ostwald-Freundlich equations for a liquid film on a soluble nanoparticle. *J Chem Phys* 2008;**129**:154116.
54. Ganta S, Paxton JW, Baguley BC, Garg S. Formulation and pharmacokinetic evaluation of an asulacrine nanocrystalline suspension for intravenous delivery. *Int J Pharm* 2009;**367**:179–86.
55. Sigfridsson K, Forssen S, Hollander P, Skantze U, de Verdier J. A formulation comparison, using a solution and different nanosuspensions of a poorly soluble compound. *Eur J Pharm Biopharm* 2007;**67**:540–7.
56. Takagi T, Ramachandran C, Bermejo M, Yamashita S, Yu LX, Amidon GL. A provisional biopharmaceutical classification of the top 200 oral drug products in the United States, Great Britain, Spain, and Japan. *Mol Pharm* 2006;**3**:631–43.
57. Li W, Zhang X, Hao X, Jie J, Tian B, Zhang X. Shape design of high drug payload nanoparticles for more effective cancer therapy. *Chem Commun* 2013;**49**:10989–91.
58. Zhang H, Hollis CP, Zhang Q, Li T. Preparation and antitumor study of camptothecin nanocrystals. *Int J Pharm* 2011;**415**:293–300.
59. Lee SE, Bairstow SF, Werling JO, Chaubal MV, Lin L, Murphy MA, et al. Paclitaxel nanosuspensions for targeted chemotherapy—nanosuspension preparation, characterization, and use. *Pharm Dev Technol* 2014;**19**:438–53.
60. Rabinow B, Kipp J, Papadopoulos P, Wong J, Glosson J, Gass J, et al. Itraconazole IV nanosuspension enhances efficacy through altered pharmacokinetics in the rat. *Int J Pharm* 2007;**339**:251–60.
61. Deng J, Huang L, Liu F. Understanding the structure and stability of paclitaxel nanocrystals. *Int J Pharm* 2010;**390**:242–9.
62. Kim S, Lee J. Folate-targeted drug-delivery systems prepared by nanocomminution. *Drug Dev Ind Pharm* 2011;**37**:131–8.
63. Liu Y, Huang L, Liu F. Paclitaxel nanocrystals for overcoming multidrug resistance in cancer. *Mol Pharm* 2010;**7**:863–9.
64. de Gracia Lux C, Joshi-Barr S, Nguyen T, Mahmoud E, Schopf E, Fomina N, et al. Biocompatible polymeric nanoparticles degrade and release cargo in response to biologically relevant levels of hydrogen peroxide. *J Am Chem Soc* 2012;**134**:15758–64.
65. Broaders KE, Grandhe S, Frechet JM. A biocompatible oxidation-triggered carrier polymer with potential in therapeutics. *J Am Chem Soc* 2011;**133**:756–8.
66. Yu SS, Koblin RL, Zachman AL, Perrien DS, Hofmeister LH, Giorgio TD, et al. Physiologically relevant oxidative degradation of oligo (proline) cross-linked polymeric scaffolds. *Biomacromolecules* 2011;**12**:4357–4366.
67. Jhaveri A, Deshpande P, Torchilin V. Stimuli-sensitive nanopreparations for combination cancer therapy. *J Control Release* 2014;**190**:352–370.
68. Shafiu Kamba A, Ismail M, Tengku Ibrahim TA, Zakaria ZA. A pH-sensitive, biobased calcium carbonate aragonite nanocrystal as a novel anticancer delivery system. *Biomed Res Int* 2013;**2013**:587451.
69. Agarwal A, Lvov Y, Sawant R, Torchilin V. Stable nanocolloids of poorly soluble drugs with high drug content prepared using the combination of sonication and layer-by-layer technology. *J Control Release* 2008;**128**:255–60.
70. Fuhrmann K, Schulz JD, Gauthier MA, Leroux JC. PEG nanocages as non-sheddable stabilizers for drug nanocrystals. *ACS Nano* 2012;**6**:1667–1676.
71. Hollis CP, Weiss HL, Evers BM, Gemeinhart RA, Li T. *In vivo* investigation of hybrid paclitaxel nanocrystals with dual fluorescent probes for cancer theranostics. *Pharm Res* 2014;**31**:1450–9.
72. Hollis CP, Weiss HL, Leggas M, Evers BM, Gemeinhart RA, Li T. Biodistribution and bioimaging studies of hybrid paclitaxel nanocrystals: lessons learned of the EPR effect and image-guided drug delivery. *J Control Release* 2013;**172**:12–21.
73. Zhao R, Hollis CP, Zhang H, Sun L, Gemeinhart RA, Li T. Hybrid nanocrystals: achieving concurrent therapeutic and bioimaging functionalities toward solid tumors. *Mol Pharm* 2011;**8**:1985–91.